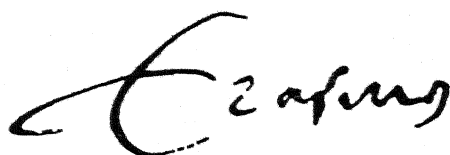


ECONOMETRIC INSTITUTE

PATTERN FORMATION FOR A
ONE DIMENSIONAL EVOLUTION EQUATION BASED ON
THOM'S RIVER BASIN MODEL

M. HAZEWINKEL, J.F. KAASHOEK AND
B. LEYNSE

REPORT 8519/B



PATTERN FORMATION FOR A ONE DIMENSIONAL EVOLUTION
EQUATION BASED ON THOM'S RIVER BASIN MODEL.*)

Michiel Hazewinkel, C.W.I. Amsterdam

Johan F. Kaashoek, Econometric Inst., Erasmus Univ. Rotterdam

Bart Leynse, Dept. Chem. Path., Erasmus Univ. Rotterdam

Abstract. A one component, one dimensional diffusion model is presented in which spatial structure is generated by means of a density dependent diffusive mechanism such that for some density values mass flow is proportional to the mass density gradient. Although stability and attractivity properties of a set of analytic periodic stationary solutions are not strong enough, the numerical work reported here, supports the possibility that this evolution equation in one space variable with zero-flux boundary conditions will have stationary attracting periodic limit distributions.

Contents

- 1. Introduction
- I.1. Thom's River Basin Model
- I.2. The Small Amplitude Scaling Continuous Limit of Thom's River Basin Equation
- II. Stationary Solutions and Stability
- II.1. Uniform Distributions
- II.2.1. Non-constant Stationary Solutions
- II.2.2. Instability of a Non-constant Solution
- III. Numerical Simulations

*) Supported by Netherlands Organization for the advancement of pure research (Z.W.O.)

1. Introduction

Pattern formation of one kind or another occurs in many systems, c.q.: star clustering (astronomy), amoebae concentrations (chemotaxis; biology), periodic precipitation (chemistry), population concentrations in cities, (spatial economy), self-fulfilling prophecies (economic behaviour). This tendency to order is even seen in some physical systems as the B nard convection shows clearly.

Since a macrosystem is described by the average density of the constituents, such cases of pattern formation can be seen as the evolution of an initial uniform distribution function to a non-uniform, well profiled function defined on the space of possible outcomes of the process (e.g.: a price distribution function in the case of self-fulfilling prophecies; spatial distribution of rising water in the case of B nard convection).

Such an evolution process can be modeled mathematically by nonlinear partial differential systems, in which "almost anything can happen", reflecting "the beauty and great variation of manifestations of the nonlinear in the bio-, geo- and other spheres around us" [4].

We mention here the so called activator-inhibitor models of Meinhardt [3]. These models are based on the possibility to distinguish between slow diffusing, growth (self-) enhancing components and fast diffusing, growth inhibiting components in the system. Since the inhibitor substance is almost uniformly present, only areas with a high activator concentration can grow further.

However, not in all cases "growth" is inhibited by some substance. For instance, an aggregation centre grows by attracting substance, at the same time causing low concentration in the neighbourhood of the centre. So the rise of new centres becomes impossible in the surroundings of already existing centres.

Apart from this depletion effect, these evolution processes are characterised by self-enhancement, also called autokatalysis. Local higher density areas themselves are the source of

amplifying fluctuations of an initial uniform ordering, for instance by gravitational instability, or economies of scale. In this paper we shall introduce a diffusion equation with density dependent diffusion coefficient, such that for some values of the density, this coefficient will be negative. This means that mass flow will be proportional to the mass concentration gradient and as such opposed at the flow direction of a Fickian diffusion. In other words: mass flow is directed towards higher concentration areas. Instability and self-amplification of fluctuations are due to this reverse diffusion. (Section I). In section II we shall give some stationary solutions of such an equation. Numerical simulations of the model are reported in section III.

As far as we know it is mathematically still an open question to show rigorously that an evolution in one space variable with zero-flux boundary conditions can have stationary attracting periodic limit distributions. The numerical work reported in this note certainly supports this possibility (as does intuition). There also are analytic periodic stationary solutions in a number of cases whose stability and attractively properties, however, are seemingly not strong enough.

I.1. Thom's river basin model

In [5] the following situation is described by Thom. Steadily rain is falling on a sandy hill; at the top brooklets are formed and destroyed almost continuously. Down the hill, the slope is less and erosion is less strong. The pattern of watersheds and brooklets becomes more stable. Remaining brooks compete with each other over the available space. The result will be an almost regular pattern at the bottom of the hill. Such pattern can be observed in nature, e.g. in Death Valley in California.

Let $s_n(t)$ denote the position of the n -th watershed (at time t). Suppose the eroding power of a stream is proportional to its basin width, then the position s_n will be governed by the following differential equation:

$$\dot{s}_n = -c(s_{n+1} - s_n) + c(s_n - s_{n-1}); c > 0 \quad (I.1)$$

(where $\dot{}$ denotes derivative with respect to t).

Any equidistant distribution with basin width a for all streams is a stationary solution of (I.1).

The character of equation (I.1) becomes clear by doing some linear stability analysis. Consider two streams with watersheds at $+a$ and $-a$, and at u near 0 on \mathbb{R} . Assuming c depends also on the basin width, we get:

$$\dot{u} = 2c(a)u + 2ac'(a)u + u^2(\dots) + \dots \quad (I.2)$$

We will have stability if $c(a) + ac'(a) < 0$.

Since erosion power will diminish at greater values of the basin width, a reasonable graph of c would be as depicted in figure (I.1)

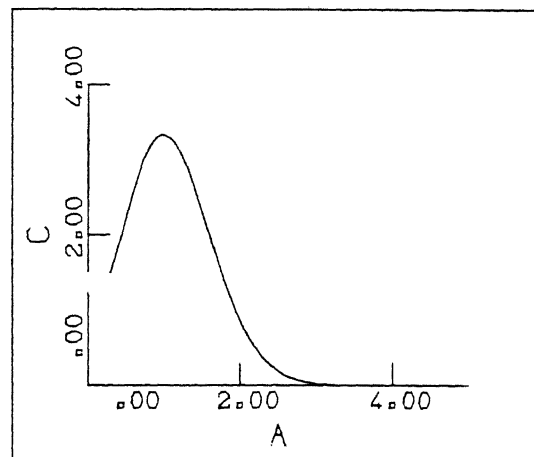


figure I.1

Then, say for $a > a_0$ with $c(a_0) + a_0c'(a_0) = 0$, stability will be obtained.

On the contrary, if stream width is in the range where $c(a) + ac'(a) > 0$, broader streams will grow at the cost of

smaller ones.

As smaller streams coincide with a higher density of the watersheds, at least in the instability range of the model, local maxima of the watersheds spatial distribution function will grow. Now at least two questions are wide open: (i) how does a more or less regular spacing of watersheds at characteristic distance a_0 arise from the initially homogeneous situation, and (ii) how does the model select between different possible a_0 . Indeed, what is observed e.g. in the Death Valley pictures alluded to above is a characteristic wave length for the spacing of the watersheds. The "equilibrium restoring force" for a spacing a_0 is $2c(a_0) + 2a_0c'(a_0)$ (< 0) and one could agree that there would be a natural tendency towards that spacing width a_0 for which this quantity $|c(a_0) + a_0c'(a_0)|$ is maximal. Other arguments favour the "largest" a_0 for which $c(a_0) + a_0c'(a_0)$ is still negative. We shall return to this question in the numerical simulation section III.

I.2. The small amplitude scaling continuous limit of the Thom's river basin equation

Let $a_n(t) = s_n(t) - s_{n-1}(t)$, $v_n(t) = \dot{s}_n(t)$ and $\phi(a) = ac(a)$, then (I.1) becomes:

$$v_n(t) = -\phi(a_{n+1}) + \phi(a_n) \quad (\text{I.3})$$

Assume ϕ is such that for $0 < \epsilon \ll 1$, $\phi(\epsilon) > \phi(a)$ for all $a > \epsilon$ then there will be functions v and a , defined on $I \times \mathbb{R}^+$,

$I = [0, L] \subset \mathbb{R}$ such that: [6]

$$v(s_n(t), t) = v_n(t) \quad (\text{I.4.1})$$

$$a\left(\frac{s_n(t) + s_{n-1}(t)}{2}, t\right) = a_n(t) \quad (\text{I.4.2})$$

Denoting the partial derivative with respect to s_n by $\frac{\partial}{\partial s_n}$, we get:

$$\begin{aligned}
a_{n+1}(t) &= a(s_n, t) \left[1 + \frac{1}{2} \frac{\partial a}{\partial n} + \frac{1}{4} \frac{\partial^2 a}{\partial n^2} + \dots \right] \\
&= a(s_n, t) \left[1 + \frac{1}{2} (-1 + \exp \frac{\partial}{\partial n}) a(s_n, t) \right]
\end{aligned} \tag{I.5.1}$$

$$\begin{aligned}
a_n(t) &= a(s_n, t) \left[1 - \frac{1}{2} \frac{\partial a}{\partial n} + \frac{1}{4} \frac{\partial^2 a}{\partial n^2} + \dots \right] = \\
&= a(s_n, t) \left[1 + \frac{1}{2} (-1 + \exp -\frac{\partial}{\partial n}) a(s_n, t) \right]
\end{aligned} \tag{I.5.2}$$

Using (I.4) and (I.5), equation (I.3) becomes (suppressing the arguments of a):

$$\begin{aligned}
v(s_n, t) = v_n(t) &= -\phi(a + \frac{1}{2} a \{(-1 + \exp \frac{\partial}{\partial n}) a\}) + \\
&+ \phi(a + \frac{1}{2} a \{(-1 + \exp -\frac{\partial}{\partial n}) a\}).
\end{aligned}$$

Take a_0 such that $\phi'(a_0) > 0$ (unstable equidistant distribution) and expand ϕ as a MacLaurin series in $a = a_0$, to find:

$$\begin{aligned}
v(s_n, t) &= -\phi'(a_0) (a - a_0 + \frac{1}{2} a \{(-1 + \exp \frac{\partial}{\partial n}) a\}) - \\
&- \frac{1}{2!} \phi''(a_0) (a - a_0 + \frac{1}{2} a \{(-1 + \exp \frac{\partial}{\partial n}) a\})^2 - \dots \\
&+ \phi'(a_0) (a - a_0 + \frac{1}{2} a \{(-1 + \exp -\frac{\partial}{\partial n}) a\}) + \\
&\frac{1}{2!} \phi''(a_0) (a - a_0 + \frac{1}{2} a \{(-1 + \exp -\frac{\partial}{\partial n}) a\})^2 + \dots
\end{aligned}$$

So we find:

$$\begin{aligned}
v(s_n, t) &= -\phi'(a_0) (a \frac{\partial a}{\partial n} + \frac{1}{3!} a \frac{\partial^2 a}{\partial n^2} + \dots) - \\
&- \frac{1}{2!} \phi''(a_0) (2(a - a_0) a \frac{\partial a}{\partial n} + \dots) + \\
&- \frac{1}{3!} \phi'''(a_0) (3(a - a_0)^2 a \frac{\partial a}{\partial n} + \dots)
\end{aligned} \tag{I.6}$$

Again using (I.4) and (I.5) one gets:

$$\begin{aligned} \frac{\partial a}{\partial t} + \frac{\partial a}{\partial n} \cdot v &= \frac{da}{dt} \approx \frac{\dot{a}_{n+1} + \dot{a}_n}{2} = \frac{v(s_{n+1}, t) - v(s_{n-1}, t)}{2} \approx \\ &\approx \frac{\partial v}{\partial n} \cdot a \end{aligned} \quad (I.7)$$

So the continuity equation for a becomes:

$$\frac{\partial a}{\partial t} = a^2 \frac{\partial(\frac{v}{a})}{\partial n} \quad (I.8)$$

Inserting (I.6) in (I.8) gives:

$$\begin{aligned} \frac{\partial a}{\partial t} &= a^2 \left[-\phi'(a_0) \left\{ \frac{\partial^2 a}{\partial n^2} + \frac{1}{3!} \frac{\partial^4 a}{\partial n^4} \right\} - \frac{1}{2} \phi''(a_0) \left\{ \frac{\partial}{\partial n} 2(a-a_0) \frac{\partial a}{\partial n} + \dots \right\} + \right. \\ &\quad \left. - \frac{1}{3!} \phi'''(a_0) \left\{ \frac{\partial}{\partial n} 3(a-a_0)^2 \frac{\partial a}{\partial n} + \dots \right\} \right] \end{aligned} \quad (I.9)$$

Now introduce a scaling factor ℓ and write $x = \ell s_n$, so that

$$\frac{\partial}{\partial n} = \ell \frac{\partial}{\partial x}.$$

Given the definition of the function a in (I.4.2), the function $\rho(x, t)$, defined by $\rho(x, t) = \frac{\ell}{a(x, t)}$, is a mass (watershed) distribution function.

Let $\rho_0 = \frac{\ell}{a_0}$ and $U(x, t) = \rho(x, t) - \rho_0$ then $a - a_0 \sim -\frac{\ell}{\rho_0} U$ and

$$\frac{\partial a}{\partial n} = -\frac{\ell^2}{\rho_0^2} \frac{\partial U}{\partial x}, \text{ so (I.9) becomes:}$$

$$\begin{aligned} \frac{\partial U}{\partial t} &= -\phi'\left(\frac{\ell}{\rho_0}\right) \left\{ \frac{\ell^4}{\rho_0^2} \frac{\partial^2 U}{\partial x^2} + \frac{\ell^6}{6\rho_0^2} \frac{\partial^4 U}{\partial x^4} \right\} + \frac{1}{2} \phi''\left(\frac{\ell}{\rho_0}\right) \cdot \\ &\quad \left\{ \frac{\ell^4}{\rho_0} \frac{\partial^2 U^2}{\partial x^2} + \dots \right\} - \frac{1}{6} \phi'''\left(\frac{\ell}{\rho_0}\right) \left\{ \frac{\ell^6}{\rho_0^6} \frac{\partial^2 U^3}{\partial x^2} + \dots \right\} \end{aligned}$$

By neglecting higher than sixth order terms in ℓ , and noting that $\phi'\left(\frac{\ell}{\rho_0}\right) > 0$, our final equation will be of the form (after an additional ρ time scaling):

$$\frac{\partial U}{\partial t} = \left[\frac{\partial^2}{\partial x^2} (-U + r_1 U^2 - r_2 U^3) - \gamma \frac{\partial^4 U}{\partial x^4} \right] \quad (I.10)$$

with $r_1 \sim \ell$, $r_2 \sim \ell^2$, $\gamma \sim \ell^2$ and $\gamma > 0$.

We take no-flux boundary conditions.

In the linear approximation (I.10) is a diffusion equation with negative diffusion coefficient; mass flux is proportional to the gradient of U . As such, equation (I.10) can be called a anti-diffusion equation stressing the fact that the flux is in the opposite direction compared to the usual normal, Fickian diffusion.

It is interesting to note that based on the Landau-Ginzburg free energy model, the same form of diffusion equation as (I.10) can be derived. In this case, the linear diffusion coefficient depends on the diffusing substance environment (e.g. Temperature) and becomes negative near the aggregative state. [1]

II. Stationary solutions and stability

We seek solutions of (I.10) in the Hilbert space $H = L^2[0,L]$ with scalar product:

$$\langle u(t), w(t) \rangle = \int_0^L U(x,t) \bar{w}(x,t) dx \quad (\text{II.1})$$

where $u(t) = U(.,t)$.

II.1. Uniform distributions:

In the Hilbert space H , equation (I.10) has the following form:

$$\frac{du}{dt} = A(\gamma)u + N(u), \quad (\text{II.2})$$

where $A(\gamma)$ is a linear operator and N is non-linear operator defined for $u = U(.)$ in a subspace of H (U must satisfy boundary conditions and $\frac{\partial U}{\partial x}$ must be square integrable). In the sequel we

suppress the variable t .

The linear operator $A(\gamma)$ is specified by:

$$[A(\gamma)u](x) = \left\{ -\frac{\partial^2 U(x)}{\partial x^2} - \gamma \frac{\partial^4 U(x)}{\partial x^4} \right\} \quad (\text{II.3})$$

Stability of the null solution $u = 0$ depends on the eigenvalues $w(\gamma)$ of $A(\gamma)$, which are entirely given by:

$$w(\gamma)U = \left\{ -\frac{\partial^2 U(x)}{\partial x^2} - \gamma \frac{\partial^4 U(x)}{\partial x^4} \right\} \quad (\text{II.4})$$

and no-flux boundary conditions, for twice continuously differentiable functions U not identically zero. Then the eigenvalues $w(\gamma)$ are:

$$w(\gamma) = \left\{ \frac{k^2 \pi^2}{L^2} - \gamma \frac{k^4 \pi^4}{L^4} \right\}, \quad k \in \mathbb{N}^+ \quad (\text{II.5})$$

with eigenvectors proportional to $\cos \frac{k\pi}{L}x$.

So the linear system would be stable if $\gamma > \frac{L^2}{\pi^2}$, and in this case

the nonlinear system is conditionally stable ([2]).

For $\gamma < \frac{L^2}{\pi^2}$, the system is unstable in one of more modes; the

fastest growing mode would be given by k such that $\frac{k^2 \pi^2}{L^2} = \frac{1}{2\gamma}$.

However, solutions (non-constant) of the linear system are

proportional to $\cos \frac{k\pi}{L}x$ with k such that $\frac{k^2 \pi^2}{L^2} = \frac{1}{\gamma}$.

Although every constant function U is a solution of (I.10), we restrict ourselves to the null solution. Since

$\rho(x,t) = \rho_0 + U(x,t)$, with $\rho_0 > 0$, constant, equation (I.10) is the evolution equation of a deviation U from a uniform distribution $\rho(x, \cdot) = \rho_0, \forall x \in I$. So stability of a uniform distribution ρ_0 is given by the stability of the null solution of

(I.10).

Note that the minus sign of the term $\frac{\partial^2 U}{\partial x^2}$ was given by

assuming $\phi'(a_0) > 0$ which coincide with instability of the original discrete Thom equations. However, with the term $\frac{\partial^4 U}{\partial x^4}$, the instability range becomes more restricted, reflecting viscosity-effects.

II.2.1. Non-constant stationary solutions

There are stationary solutions of

$$\frac{\partial U}{\partial t} = \left\{ \frac{\partial^2}{\partial x^2} (-U + r_1 U^2 - r_2 U^3) - \gamma \frac{\partial^4 U}{\partial x^4} \right\} \quad (\text{II.6})$$

with $r_1 \sim \ell$; $r_2 \sim \ell^2$; $\gamma \sim \ell^2$, which can be obtained as follows. Consider:

$$U(x) - r_1 U^2(x) + r_2 U^3(x) + \gamma \frac{d^2 U}{dx^2} = \text{Constant} \quad (\text{II.7})$$

If $U(x)$ also satisfies the boundary conditions, then it will be a stationary solution of (II.6).

There are solutions of the form:

$$U_0(x) = \frac{1}{\alpha + \beta \cos \frac{k\pi}{L} x} \quad (\text{II.8})$$

$$\text{with } r_1 = 3\alpha; r_2 = 2(\alpha^2 - \beta^2) \text{ and } \gamma \cdot \left(\frac{k\pi}{L}\right)^2 = 1 \quad (\text{II.9})$$

These yields bounded solutions only if $r_2 > 0$. Note that one can solve for α, β, k in terms of r_1, r_2, γ . (We shall mention other solutions at the end of this section). Since we conceive of equation (I.10) as the evolution equation of a disturbance U of a uniform distribution, (II.8) can not be taken as a solution of (I.10). Given the boundary conditions, one must have:

$$\int_0^L U_0(x) dx = 0.$$

Let $V_0(x) = U_0(x) - d$, with $U_0(x)$ as in (II.8) and

$$d = \frac{1}{L} \int_0^L U_0(x) dx.$$

Then $V_0(x)$ will be a solution of:

$$V(x) - r_1^* V^2(x) + r_2^* V^3(x) - \gamma^* \frac{d^2 V}{dx^2} = \text{Constant} \quad (\text{II.10})$$

with

$$r_1^* = \frac{r_1 - 3r_2 d}{1 - 2r_1 d + 3r_2 d^2}$$

$$r_2^* = \frac{r_2}{1 - 2r_1 d + 3r_2 d^2}$$

$$\gamma^* = \frac{\gamma}{1 - 2r_1 d + 3r_2 d^2}$$

Since $d = \frac{1}{\sqrt{\alpha^2 - \beta^2}} \sim \frac{1}{\ell}$, all the coefficients of (II.10) are of the

same order in ℓ , as in equation (I.10). So $V_0(x)$ will be a proper solution of equation (I.10) with coefficients r_1^* , r_2^* and γ^* . This solution has a different wave length than a solution in the

linear case (see section II.1 with $\gamma^* \frac{k^2 \pi^2}{L^2} = 1$).

And definitely, the term $\frac{\partial^4 U}{\partial x^4}$ models "viscosity"-effects. If γ^*

tends to zero, the wave length becomes infinitely small and there is no coherence at all between the mass particles (watersheds!). In the other limit case, $\gamma^* \rightarrow \infty$, V_0 tends to the null solution (Any uniform distribution is stable!).

Before reporting on the stability of the solution $V_0(x)$, we mention other stationary solutions of (II.6):

$$i) U(x) = \frac{1}{\alpha + \beta \cos^2\left(\frac{k\pi}{L}x\right)} \text{ with: } r_1 = \frac{3}{2}\alpha; r_2 = 2\alpha(\alpha + \beta); \gamma \cdot \frac{k^2\pi^2}{L^2} = \frac{1}{4}$$

(This solution belongs to the above mentioned family of solutions.)

$$ii) U(x) = \frac{1}{\alpha + \beta_1 \cos\frac{k\pi}{L}x + \beta_2 \cos^3\left(\frac{k\pi}{L}x\right)} \quad (II.11)$$

$$\text{with } r_1 = 3\alpha; r_2 = 2\left(\alpha^2 - \frac{1}{9}\beta_1^2\right); \gamma \frac{k^2\pi^2}{L^2} = \frac{1}{9}; \beta_2 = -\frac{4}{3}\beta_1. \quad (II.12)$$

$$iii) U(x) = \frac{1}{\alpha + \beta_1 \cos^2\left(\frac{k\pi}{L}x\right) + \beta_2 \cos^4\left(\frac{k\pi}{L}x\right)} \quad (II.13)$$

$$\text{with } r_1 = 3\alpha + \frac{3}{8}\beta_1; r_2 = 2\left(\alpha^2 + \frac{1}{4}\alpha\beta_1\right); \gamma \cdot \frac{k^2\pi^2}{L^2} = \frac{1}{16}; \beta_2 = -\beta_1.$$

These solutions are bounded only if $r_2 > 0$.

Of related interest are solutions of:

$$U(x) + r_2 U^3(x) + r_4 U^5(x) + \gamma \frac{d^2 U}{dx^2} = 0.$$

which are of the form

$$U(x) = \frac{1}{\sqrt{\alpha + \beta \cos\frac{k\pi x}{L}}}, \quad (II.14)$$

$$\text{with } r_2 = -4\alpha (< 0!), \gamma \cdot \frac{k^2\pi^2}{L^2} = 4 \text{ and } \alpha^2 > \beta^2 \text{ if } r_4 > 0.$$

II.2.2. Instability of a non-constant solution

In this section we investigate the stability of a solution $V_0(x)$ of equation (II.10) as derived in II.2.1.

Since $V_0(x) = U_0(x) - d$, with $U_0(x)$ is a solution of (II.7), resp. a stationary solution of (II.6), and the connection between the coefficients of (II.10) and (II.6), stability of $V_0(x)$ follows from stability of $U_0(x)$ and vice versa.

Let $W(x, t)$ be a disturbance of $U_0(x)$, then:

$$\frac{\partial W}{\partial t} = \left\{ \frac{\partial^2}{\partial x^2} (-1 + 2r_1 U_0(x) - 3r_2 U_0^2(x)) W - \gamma \frac{\partial^4 W}{\partial x^4} \right\} + \text{non-linear terms in } W \quad (\text{II.15})$$

with no-flux boundary conditions.

And $U_0(x)$ will be stable if the null solution $W(.,.) \equiv 0$ is a stable solution of (II.15)

As in section II.1, we can write down (II.15) in the Hilbert space H , and now the linear operator $A(\gamma)$ is specified as:

$$[A(\gamma)w](x) = \left\{ \frac{\partial^2}{\partial x^2} (-1 + 2r_1 U_0(x) - 3r_2 U_0^2(x)) W(x) - \gamma \frac{\partial^4 W(x)}{\partial x^4} \right\}$$

with $w(.) \in H$; $w(.) = W(x, .)$.

However, eigenvalues of $A(\gamma)$ are not found, so linear stability cannot be established along this way.

Denoting $2r_1 U_0(x) - 3r_2 U_0^2(x)$ by $f(x)$, then

$$f(x) = \frac{6\delta}{\delta + \cos \frac{k\pi x}{L}} - \frac{6(\delta^2 - 1)}{(\delta + \cos \frac{k\pi x}{L})^2} \quad (\text{II.16})$$

where $\delta = \frac{\alpha}{\beta}$ and $\frac{k\pi}{L} = \sqrt{\frac{1}{\gamma}}$ (see (II.9)).

Define in H the functional $F(t)$ by:

$$[F(t)]w = \int_0^L W^2(x, t) dx = \|w\|_2^2 \quad (\text{II.17})$$

Then $[F(t)]w = 0 \rightarrow w = 0$ and $\frac{dF}{dt}(w) = \int_0^L 2W(x, t) \frac{\partial W}{\partial t} dx$.

Now using only the linear part of (II.15.1), then by partial integration,

$$\frac{dF}{dt}(w) = 2 \left[\int_0^L \left(\frac{\partial W}{\partial x} \right)^2 dx - \gamma \int_0^L \left(\frac{\partial^2 W}{\partial x^2} \right)^2 dx + \int_0^L f(x) W(x, t) \frac{\partial^2 W}{\partial x^2} dx \right] \quad (\text{II.18})$$

If we take $W(x, .)$ proportional to $\cos \frac{k\pi x}{L}$ (with $\frac{k\pi}{L} = \sqrt{\frac{1}{\gamma}}$) then (II.18) reduces to:

$$\frac{dF}{dt}(w) = 2 \int_0^L f(x) W(x, t) \frac{\partial^2 W}{\partial x^2} dx \quad (\text{II.19})$$

And in this case (W proportional to $\cos \frac{k\pi x}{L}$), $\frac{dF}{dt} > 0$ if

$$\int_0^L f(x) \cos^2\left(\frac{k\pi x}{L}\right) dx < 0 \quad (\text{II.20})$$

(II.20) is equivalent with:

$$6 - 12\delta^2 + 12\delta\sqrt{\delta^2 - 1} < 0 \quad (\text{II.21})$$

which holds for any δ , with $\delta^2 \geq 1$ ($\delta^2 = \frac{\alpha^2}{\beta^2} > 1$ if $r_2 > 0$).

Since F gives the norm of w , and w with $w(\cdot) = W(x, \cdot)$ proportional to $\cos\frac{k\pi x}{L}$ can be taken as close in norm to $w = 0$ as one wishes, $\frac{dF}{dt} > 0$ means linear unstability of the solution $U_0(x)$ (in L_2 -norm).

So the solution $V_0(x)$ is unstable.

III Numerical simulations

We have made numerical simulations of

$$\frac{\partial U}{\partial t} = \frac{\partial^2}{\partial x^2} \phi(U) - \gamma \frac{\partial^4 U}{\partial x^4} \quad (\text{III.1})$$

$$\text{where } \phi(U) = -U + r_1 U^2 - r_2 U^3 \quad (\text{III.2})$$

defined on the interval $[0, L] \subset \mathbb{R}$ with no-flux boundary conditions.

III.1 Case $r_2 > 0$

The stationary solutions of section II.2 are never found numerically. Even if the initial value is a discretization of such a non-constant solution, in time the solution becomes unbounded. Since these solution are unstable, another outcome could not be expected

III.2 Case $r_2 < 0$

III.2.1. $\gamma = 0$

If $\gamma = 0$ the discretization of (III.1) gives a set of equations

similar to Thom's original model.

The null solution is unstable and the smallest possible wavelength mode grow fastest. The final pattern is characterised by two constant values U_0 and U_1 with:

$$U_0 \neq U_1; \phi(U_0) = \phi(U_1); \phi'(U_0) = \phi'(U_1) > 0 \quad (\text{III.3})$$

In figure III.1, $r_1 = 0$, $r_2 = -\frac{1}{3}$ and $U_0 = \sqrt{3}$, $U_1 = -\sqrt{3}$

In figure III.2, $r_1 = -\frac{4}{5}$, $r_2 = -\frac{1}{5}$ and $U_0 = \frac{4+\sqrt{93}}{3}$, $U_1 = \frac{4-\sqrt{93}}{3}$
Typical block-like solutions can be generated also (figure III.3.6).

The values U_0 and U_1 are in the following way deduced.

First we note that solutions of (III.1) are independent of transformations: $\phi(U) \rightarrow \phi(U) + C_0$, with C_0 some constant. Given the boundary conditions, stationary solutions of (III.1) with $\gamma = 0$ are given by:

$$\phi(U) = \beta \text{ and } \int_0^L U(x)dx = 0 \quad (\text{III.3})$$

or equivalently:

$$V(U) = \beta U + \alpha \text{ and } \int_0^L U(x)dx = 0 \quad (\text{III.4})$$

where $V(U) = \int_0^U \phi(s)ds$ and α, β constants.

Define on $L^2[0, L]$, the functional $F(t)$:

$$[F(t)](U) = \int_0^L V(U)dx \quad (\text{III.5})$$

Now differentiating F with respect to t , we find by partial integration:

$$\frac{dF}{dt} = \int_0^L - \left(\frac{\partial \phi(U)}{\partial x} \right)^2 dx \quad (\text{III.6})$$

So, $\frac{dF}{dt} \leq 0$ and $\frac{dF}{dt} = 0$ if and only if U is a stationary solution $\phi(U) = \beta$.

Further, by variational methods, the first order condition for extreme points of:

$$\int_0^L V(U)dx + \lambda \int_0^L U(x)dx \quad (\text{III.6})$$

$$\text{is } \phi(U) = -\lambda, \int_0^L U(x)dx = 0.$$

Using (III.4) the value of (III.6) at these points is given by:

$$\int_0^L \alpha dx \quad \text{subject to } \int_0^L U(x)dx = 0 \quad (\text{III.7})$$

Now using ϕ is cubic in U , we find:

if $r_2 > 0$: $\int_0^L \alpha dx$ has an absolute (bounded) maximum value and is unbounded from below.

if $r_2 < 0$: $\int_0^L \alpha dx$ has an absolute (bounded) minimum value and is unbounded from above.

These bounded extreme values are attained for stationary solutions characterised by only two values U_0 and U_1 , such that:

$$\phi(U_0) = \phi(U_1) \quad (\text{III.8})$$

$$\phi'(U_0) = \phi'(U_1) = \begin{cases} < 0 & \text{if } r_2 > 0 \\ > 0 & \text{if } r_2 < 0 \end{cases} \quad (\text{III.9})$$

(if ϕ is cubic in U).

Combining (III.6), (III.8) and (III.9) give that, for $r_2 < 0$ a solution of the form:

$$U(x) = U_0 + H(x-x_0)(U_1-U_0)$$

with $H(x-x_0)$ is Heaviside function, will be conditional stable if

U_0, U_1 satisfy (III.8) and (III.9). ($x_0 = \frac{LU_1}{U_1-U_0}$).

III.2.2. $\underline{\gamma \neq 0}$

In this case we can choose γ such that the null solution is unstable in modes with wavelength bounded away from zero. The pattern evolution is dominated initially by the mode $\cos \frac{k\pi x}{L}$

with $\frac{k^2 \pi^2}{L^2} = \frac{1}{2\gamma}$ (see section II.1).

In figure III.3a, the pattern evolution is shown for $r_1 = 0$, $r_2 = -\frac{1}{3}$ and $\gamma = 0,00482$; the largest positive eigenvalue is for $k = 16$ which corresponds to a wavelength $\sim 0,6$ (e.h.) in figure III.3. The final pattern shows a wavelength which is at least twice as long. The same holds for other values of γ ; in figure III.4 we have taken $\gamma = 0,00241$ (largest eigenvalue for $k = 24$, wavelength $\sim 0,4$ (e.h.)); figure III.5: $\gamma = 0,01563$ (largest eigenvalue for $k = 9$, wavelength $\sim 1,1$ (e.h.)).

In figure III.6, $r_1 = -\frac{4}{5}$, $r_2 = -\frac{1}{5}$, $\gamma = 0,01563$. Compared with figure III.5, the difference must be a consequence of the fact that the number of gridpoints with $U_0 = \frac{4+\sqrt{93}}{3}$ (figure III.2) is far less than the number of gridpoints with $U_0 = \sqrt{3}$ (figure III.1) which are the corresponding figures if $\gamma = 0$.

In figure III.3b, we have set $\gamma = 0$ after reaching the final pattern as depicted in III.3a. The final block form is totally given by the values U_0 and U_1 as derived in section III.2.1.

We conclude this section with a simulation of the following model:

$$\frac{\partial \rho}{\partial t} = \frac{\partial^2}{\partial x^2} \phi(1/\rho) - \gamma \frac{\partial^4 \rho}{\partial x^4} \quad (\text{III.9})$$

defined on $[0, L] \times \mathbb{R}^+$, with no-flux boundary conditions.

Equation (III.9) is derived from Thom's model without expanding ϕ in a MacLaurin series. We have taken ϕ cubic like:

$$\phi(a) = 0,16 \left\{ (1+a)e^{-a/8} + \frac{0,25}{a} \right\}.$$

Initial value ρ_0 and γ is taken such that in linear approximation equation (III.9) corresponds with the equation belonging to figure III.4. The pattern evolution is shown in figure III.7. Depicted is the scaled variable s , defined by $\rho = \rho_0(1+s)$. As expected from the foregoing analysis, the final patterns in figure III.4 and III.7 are quite different.

We note further that at every stage of the evolution s is greater than minus one which is appropriate for this scaled density function. This can always be achieved by choosing the cubic diffusion term ϕ , as function of s , such that $\phi(-1)$ is less than the local minimum value of ϕ , which is the same condition as in section I.2.

III.3. Figures

Figure III.1: $\phi(U) = -U + \frac{1}{3}U^3$; $\gamma = 0$

Figure III.2: $\phi(U) = -U - \frac{4}{5}U^2 + \frac{1}{5}U^3$; $\gamma = 0$

Figure III.3: $\phi(U) = -U + \frac{1}{3}U^3$; $\gamma = 0,00482$

III.3a: dotted curve initial evolution pattern; continuous curve final pattern.

III.3b: after setting $\gamma = 0$, the final pattern of figure III.3a becomes block-like.

Figure III.4: $\phi(U) = -U + \frac{1}{3}U^3$; $\gamma = 0,00241$.

Figure III.5: $\phi(U) = -U + \frac{1}{3}U^3$; $\gamma = 0,01563$

dotted curve: initial pattern;
continuous curve: final pattern.

Figure III.6: $\phi(U) = -U - \frac{4}{5}U^2 + \frac{1}{5}U^3$; $\gamma = 0,01563$

Figure III.7: $\phi(U) = 0,16\left\{(1+U)e^{-U/8} + \frac{0.25}{U}\right\}$; $\gamma = 0,00482$

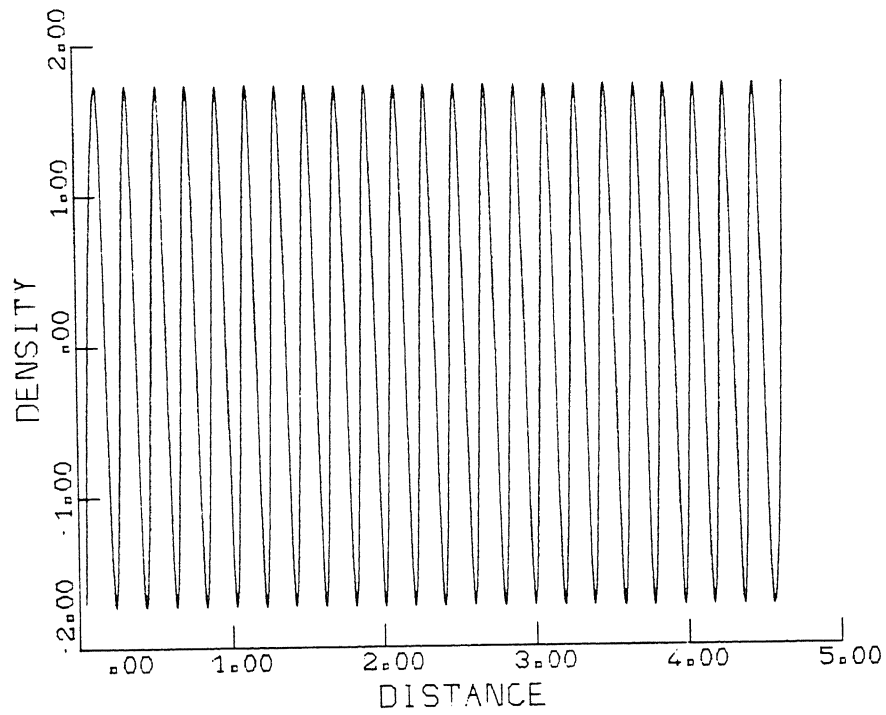


Figure III.1: $\phi(U) = -U + \frac{1}{3}U^3$; $\gamma = 0$

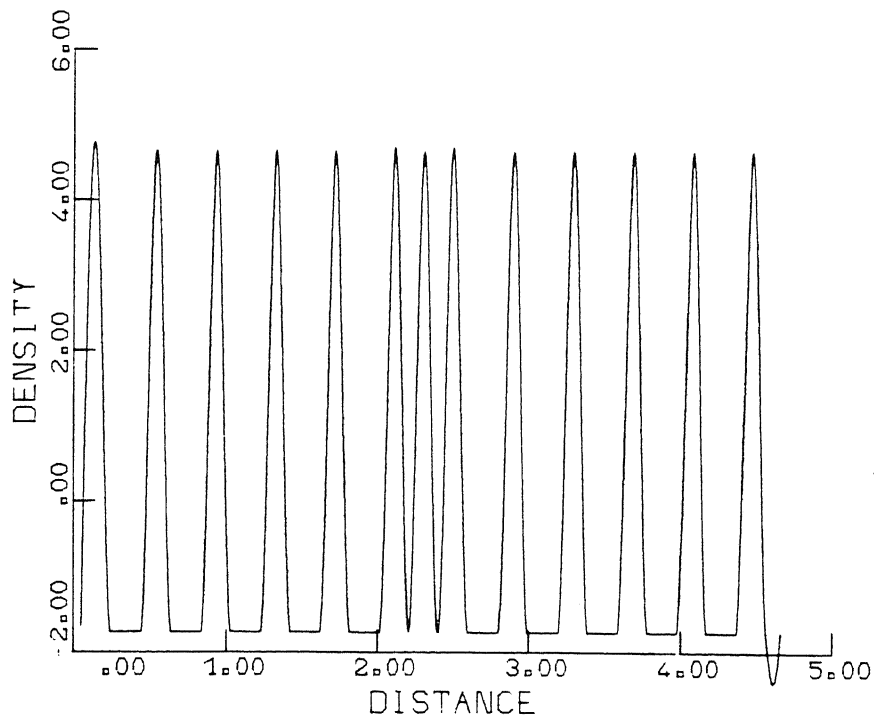


Figure III.2: $\phi(U) = -U - \frac{4}{5}U^2 + \frac{1}{5}U^3$; $\gamma = 0$

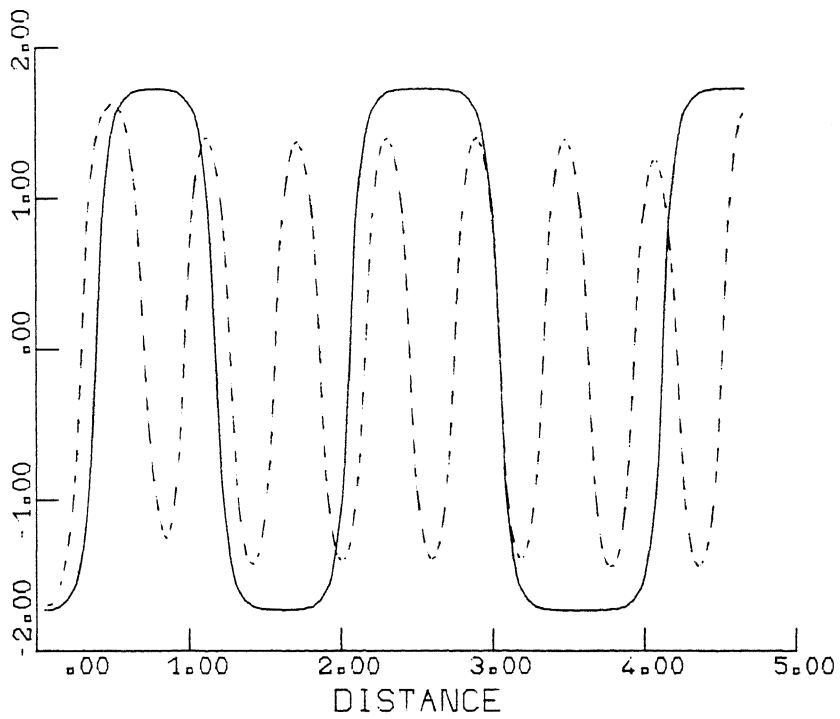


Figure III.3a: $\phi(U) = -U + \frac{1}{3}U^3$; $\gamma = 0,00482$
 Final pattern: continuous curve

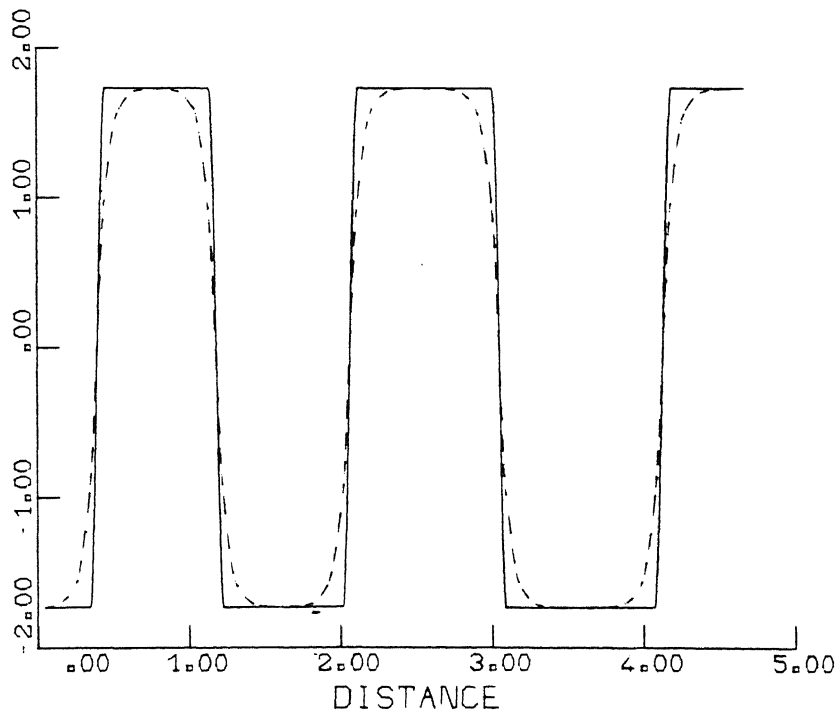


Figure III.3b: Continuation of final pattern of (III.3a) after setting $\gamma = 0$.

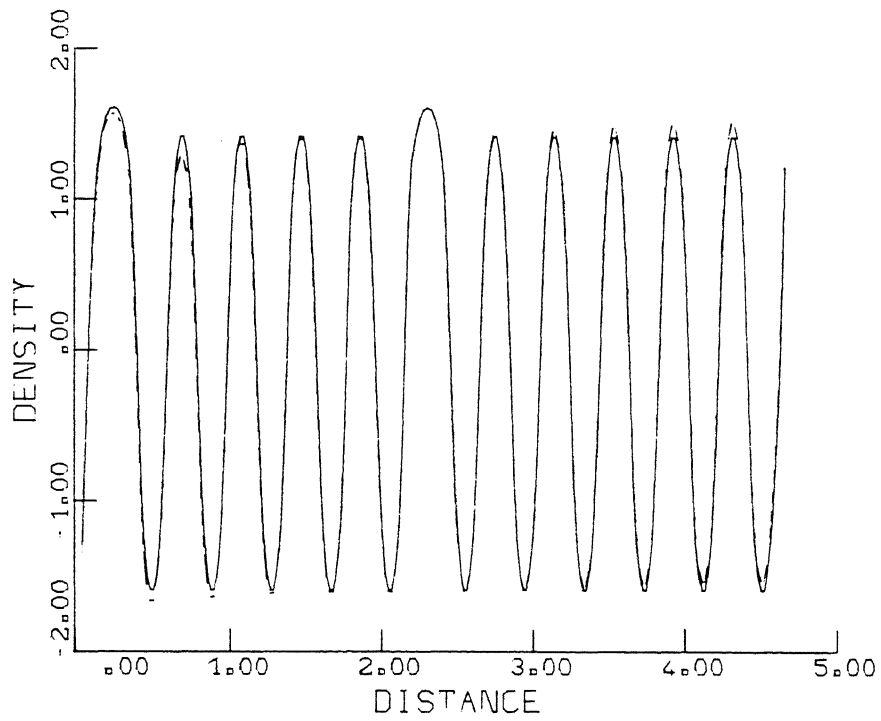


Figure III.4: $\phi(U) = -U + \frac{1}{3}U^3$; $\gamma = 0,00241$.

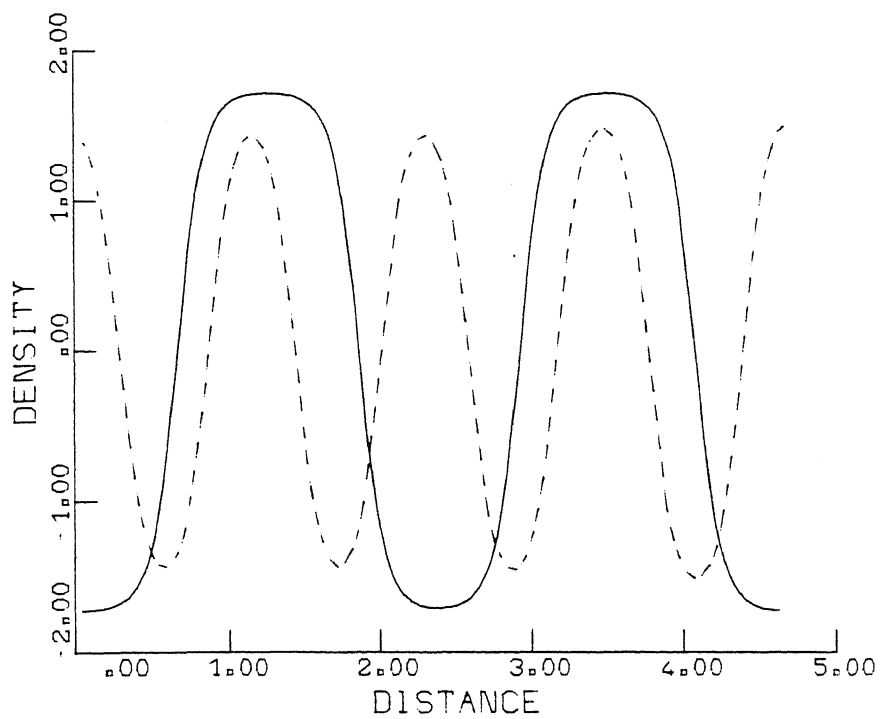


Figure III.5: $\phi(U) = -U + \frac{1}{3}U^3$; $\gamma = 0,01563$

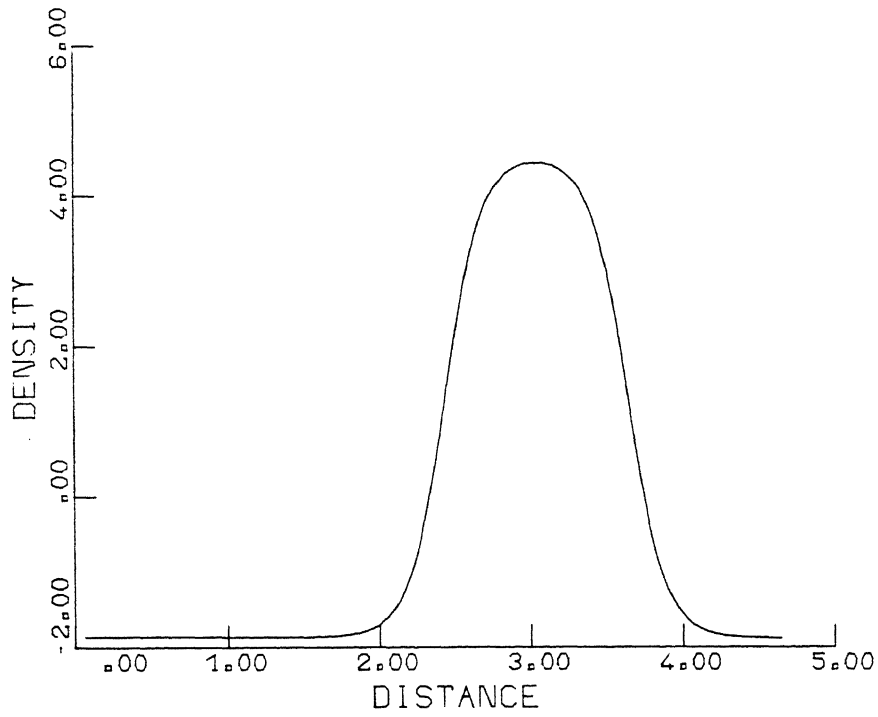


Figure III.6: $\phi(U) = -U - \frac{4}{5}U^2 + \frac{1}{5}U^3$; $\gamma = 0,01563$.

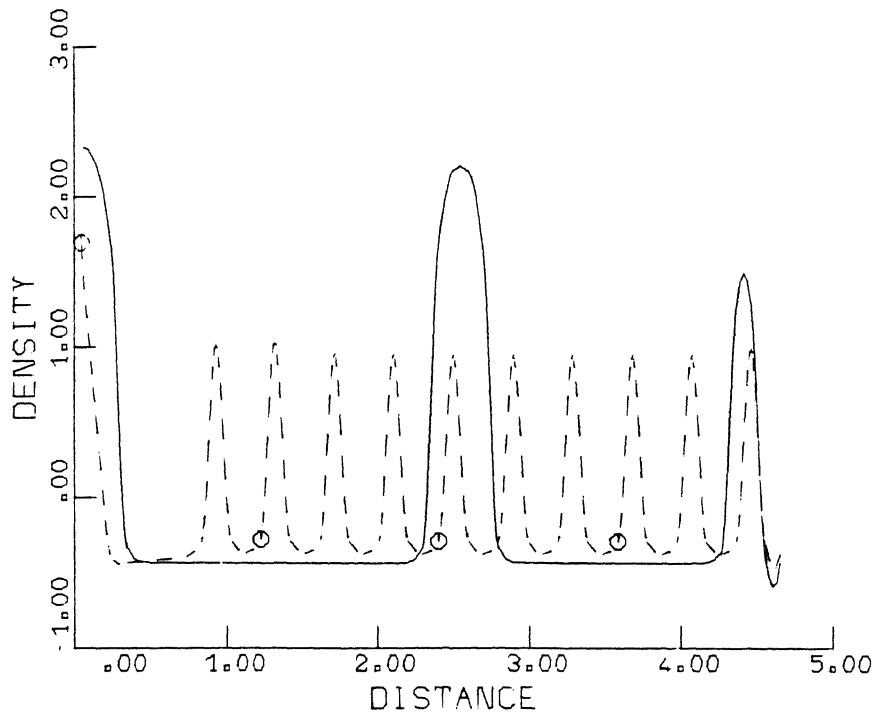


Figure III.7: $\phi(U) = 0,16\left\{(1+U)e^{-\frac{U}{8}} + \frac{0,25}{U}\right\}$; $\gamma = 0,00482$.

Conclusion

Thom's river basin model describes the situation in which for a certain basin width, large basins grow at the cost of smaller ones. In defining a continuous distribution function for the watersheds of the basins, we have derived an evolution equation of pure diffusion type. The diffusion coefficient is density dependent and negative for some range of density values. In deriving this continuous form of Thom's discrete model, it is quite natural to incorporate a fourth order derivative term which can be interpreted as modelling viscosity effects.

We have found a class of stationary solutions of this so-called anti-diffusion equation, which are, however, not stable. If the diffusion term is of cubic form with two stable branches, numerically we have found bounded non-constant solutions. By deleting the fourth order derivative term, the solution becomes block form like and is totally characterised by two unique density values.

As such, this anti-diffusion equation seems a respectable candidate for modelling evolution processes which form patterns in the case that there is only one substance involved.

References

1. Cohen, D.S. and Murray, J.D.: 'A generalized diffusion model for growth and dispersal in a population', *Journal of Mathematical Biology* 12 (1981), 237-249.
2. Iooss, G. and Joseph, D.D.: Elementary stability and bifurcation theory, Springer-Verlag, New York, 1980.
3. Meinhardt, H.: 'The Spatial Control of Cell Differentiation by Autocatalysis and Lateral Inhibition', in H. Haken (ed), Synergetics, a workshop, Springer-Verlag Berlin, 1977.
4. Ortoleva, P.: 'The Multifaceted Family of the Nonlinear: Waves and Fields, Center Dynamics, Catastrophes, Rock Bands and Precipitation Patterns', in A. Pacault and C. Vidal (eds.),

Synergetics, Far from Equilibrium, Springer-Verlag Berlin, 1979.

5. Thom, R.: 'Symmetries gained and lost', in K. Maurin and R. Raczka (eds.), Mathematical physics and physical mathematics, Reidel, Dordrecht, 1976.
6. Whitman, G.B.: Linear and Nonlinear Waves, Wiley-Interscience New York, 1974.